

Supporting Information

Functionalization of BaTiO₃ Nanoparticles with Electron Insulating and Conducting Organophosphazene-based Hybrid Materials

George S. Pappas¹, Chaoying Wan^{1*}, Chris Bowen², David M. Haddleton³, Xiaobin Huang⁴

¹*International Institute for Nanocomposites Manufacturing (IINM), WMG, University of Warwick, CV4 7AL, UK*, ²*Materials and Structures Centre, Department of Mechanical Engineering, University of Bath, BA2 7AY, UK*, ³*Department of Chemistry, University of Warwick, CV4 7AL, Coventry, UK*, ⁴*School of Aeronautics and Astronautics, Shanghai Jiao Tong University, 200240, P. R. China*

Table S1. Concentrations of BPS, HCCP and BaTiO₃ for forming OPZ@BaTiO₃

Sample name [Shell@Core]	BaTiO ₃ to monomers weight ratio	BPS (mg/ml)	HCCP (mg/ml)	BaTiO ₃ (mg/ml)
OPZ@BaTiO ₃ -0.25	0.25:1	0.81	0.36	4.65
OPZ@BaTiO ₃ -0.5	0.5:1	1.45	0.64	4.15
OPZ@BaTiO ₃ -1	1.33:1	1.39	0.61	1.50
OPZ@ BaTiO ₃ -4	4:1	4.17	1.83	1.50
OPZ nanospheres	-	1.13	2.57	-

Table S2. Weight percentages as calculated from EDS analysis.

	C	O	S	P	N	Cl	Ba	Ti
Sample	weight %							
OPZ@BaTiO ₃ -0.25	9.4	19.2	1.0	1.3	0.3	0.5	51.0	17.3
OPZ@BaTiO ₃ -0.5	20.0	25.5	1.8	2.1	0.5	0.6	39.1	13.5
OPZ@BaTiO ₃ -1	25.1	31.9	2.1	2.8	1.4	1.3	26.5	8.9
OPZ@BaTiO ₃ -4	36.0	18.5	4.1	4.6	3.8	1.3	24.6	7.0
C@BaTiO ₃ -0.25	2.7	6.7	0.3	1.3	0.1	0.2	65.5	23.4
C@BaTiO ₃ -0.5	4.8	6.6	0.3	1.2	0	0.2	56.5	20.3
C@BaTiO ₃ -1	29.0	16.7	1	5.5	0.4	0	36.0	10.7
C@BaTiO ₃ -4	54.6	14.0	2.1	8.5	4.1	0	12.6	4.1

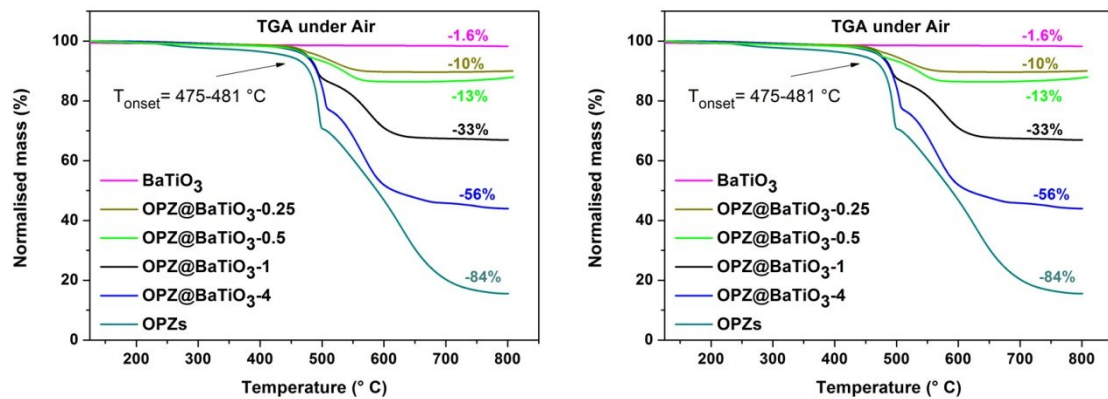


Figure S1. TGA curves under air of the a) OPZ@BaTiO₃ the bare BaTiO₃ nanoparticles and b) C@BaTiO₃. The mass loss was calculated at the range 120–700°C.

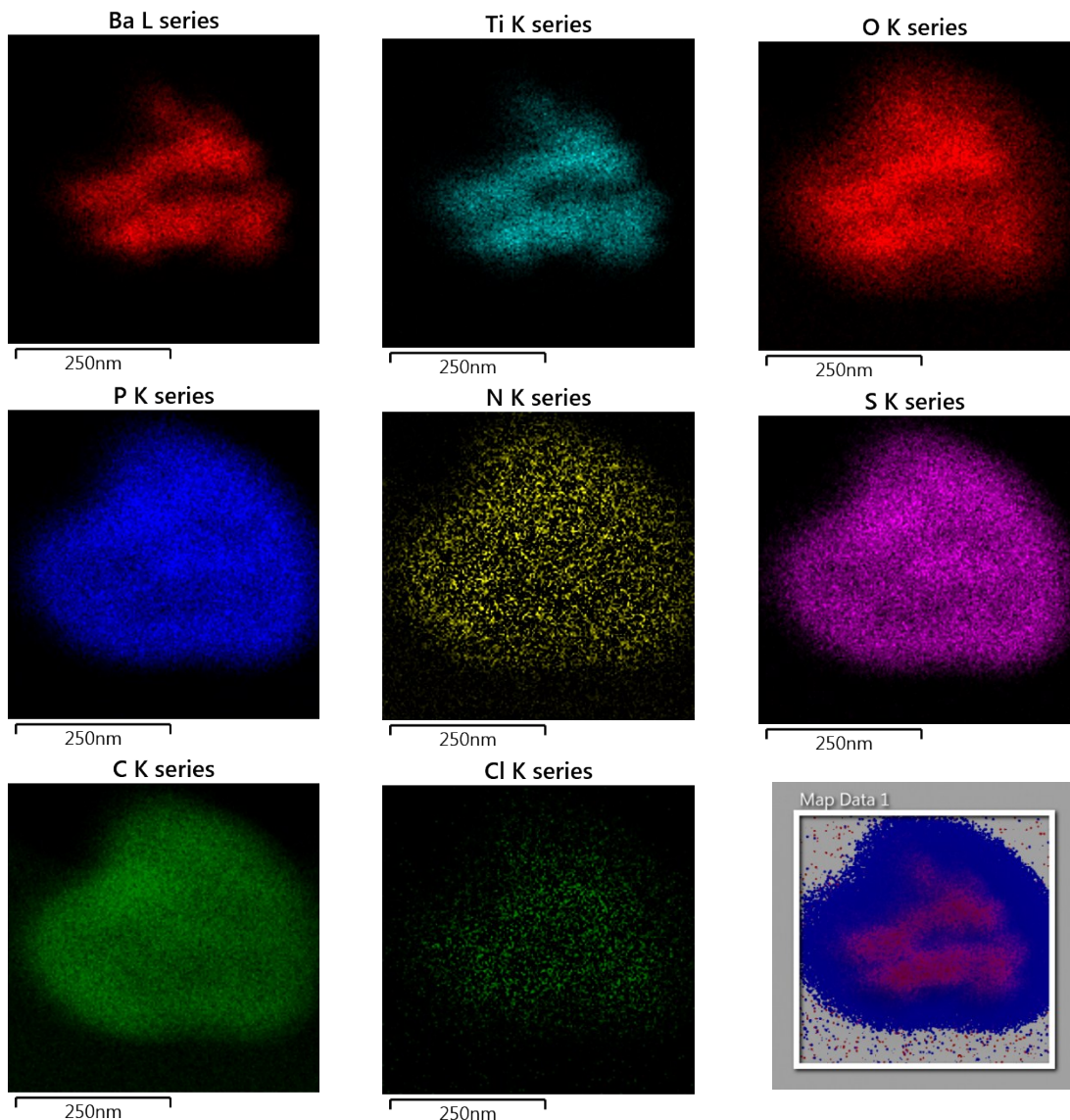


Figure S2. TEM-EDX elemental mapping of the OPZ@BaTiO₃-4 a) individual mapping of all the elements and the overlay mapping of the Ba (core) and P (shell).

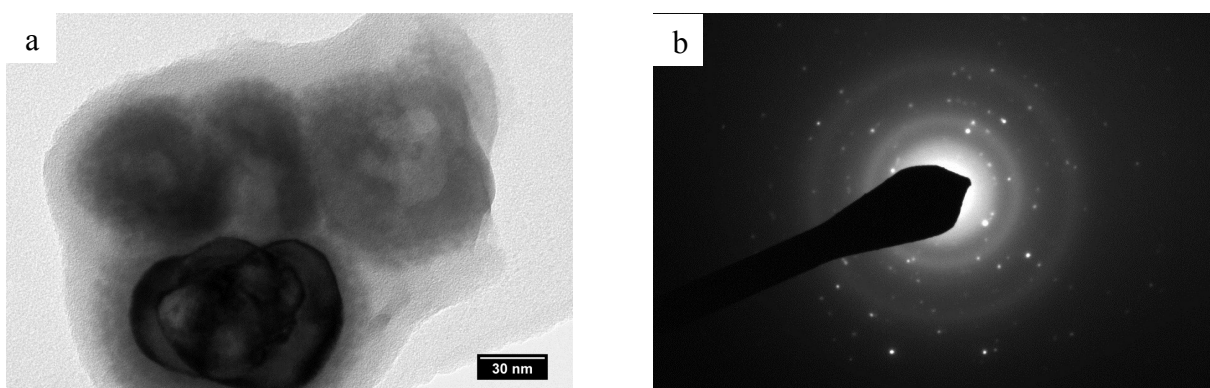


Figure S3. a) TEM micrograph of the C@BaTiO₃-1 and b) the corresponding SAED pattern.

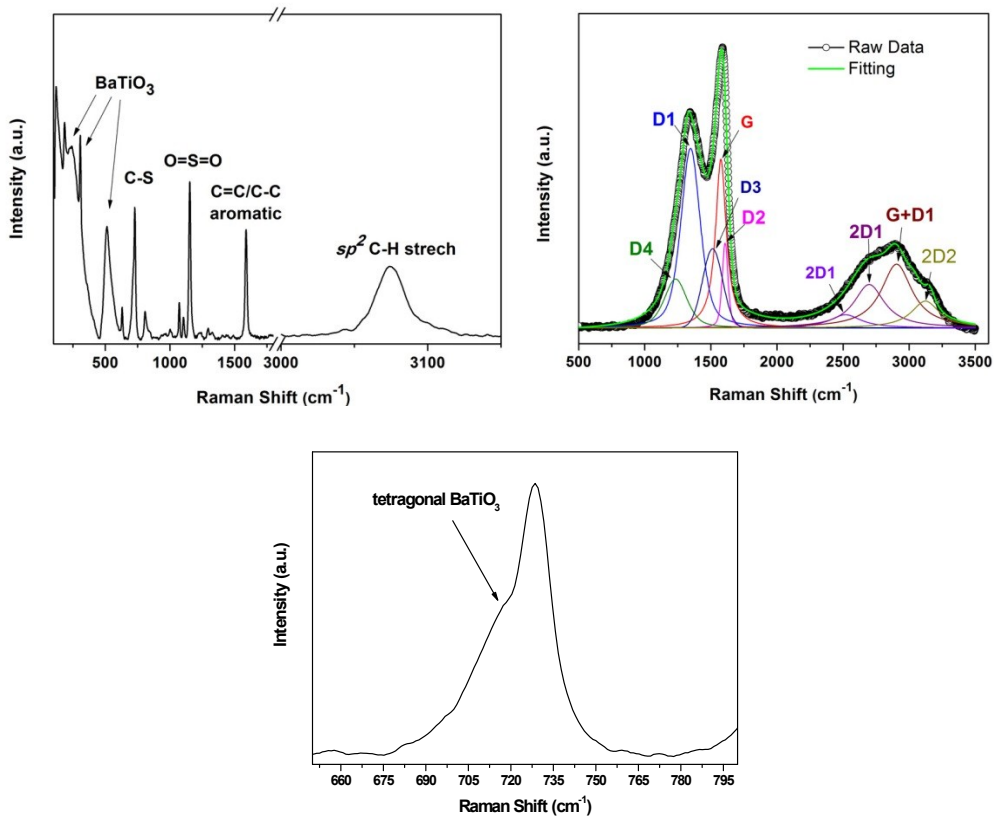


Figure S4. Characteristic Raman spectra of a) OPZs@ BaTiO₃-1 and b) C@ BaTiO₃-1, Raman spectra of the OPZ@BaTiO₃ highlighting the presence of the tetragonal structure of BaTiO₃.

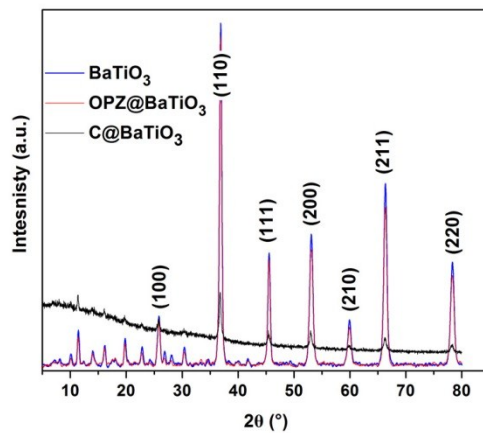


Figure S5. XRD patterns of BaTiO₃, OPZ@BaTiO₃ and C@BaTiO₃.

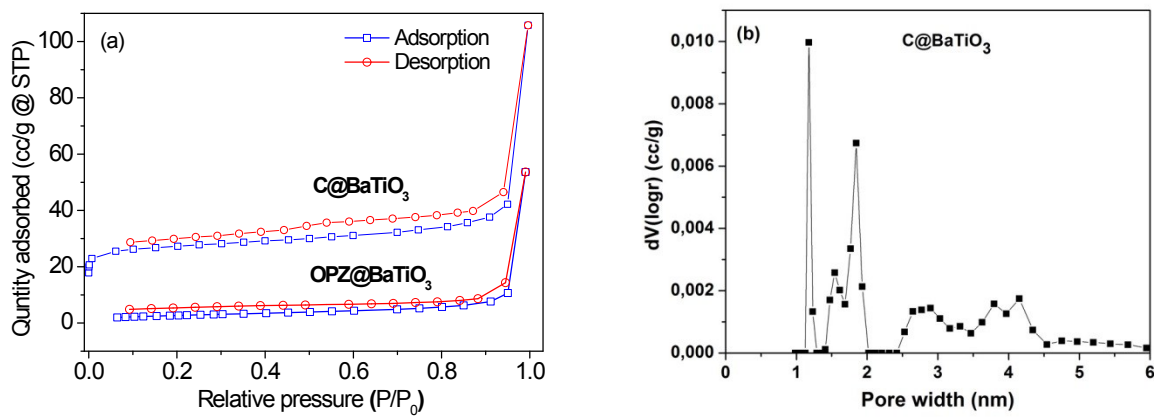


Figure S6. Representative a) N_2 adsorption-desorption isotherms of the core-shell particles before and after carbonization and b) pore size distribution of the $C@BaTiO_3$ samples based on NLDFT calculation.

Table S3. Textural properties of the samples calculated from N₂ sorption isotherms

Sample name [Shell@Core]	Specific surface area m ² /g	Micropore area m ² /g
OPZ@BaTiO ₃ -0.25	34	0
OPZ@BaTiO ₃ -0.5	19	0
OPZ@BaTiO ₃ -1	10	0
OPZ@BaTiO ₃ -4	9	0
C@BaTiO ₃ -0.25	34	5
C@BaTiO ₃ -0.5	65	13
C@BaTiO ₃ -1	105	21
C@BaTiO ₃ -4	183	153

Table S4. Percentage atomic concentrations as calculated from high resolution XPS analysis

	C 1s	O 1s	S 2p	P 2p	N 1s	Cl 2p	Ba 3d	Ti 2p
Sample	atomic %							
OPZ@BaTiO ₃ -1	63.05	21.94	5.13	5.81	3.72	0.58	0.34	0.37
OPZ@BaTiO ₃ -4	63.12	21.30	5.16	5.24	4.37	0.81	-	-
C@BaTiO ₃ -1	82.43	10.59	0.89	2.21	1.82	-	1.71	0.35
C@BaTiO ₃ -4	82.93	9.86	1.24	3.01	2.69	-	0.28	-

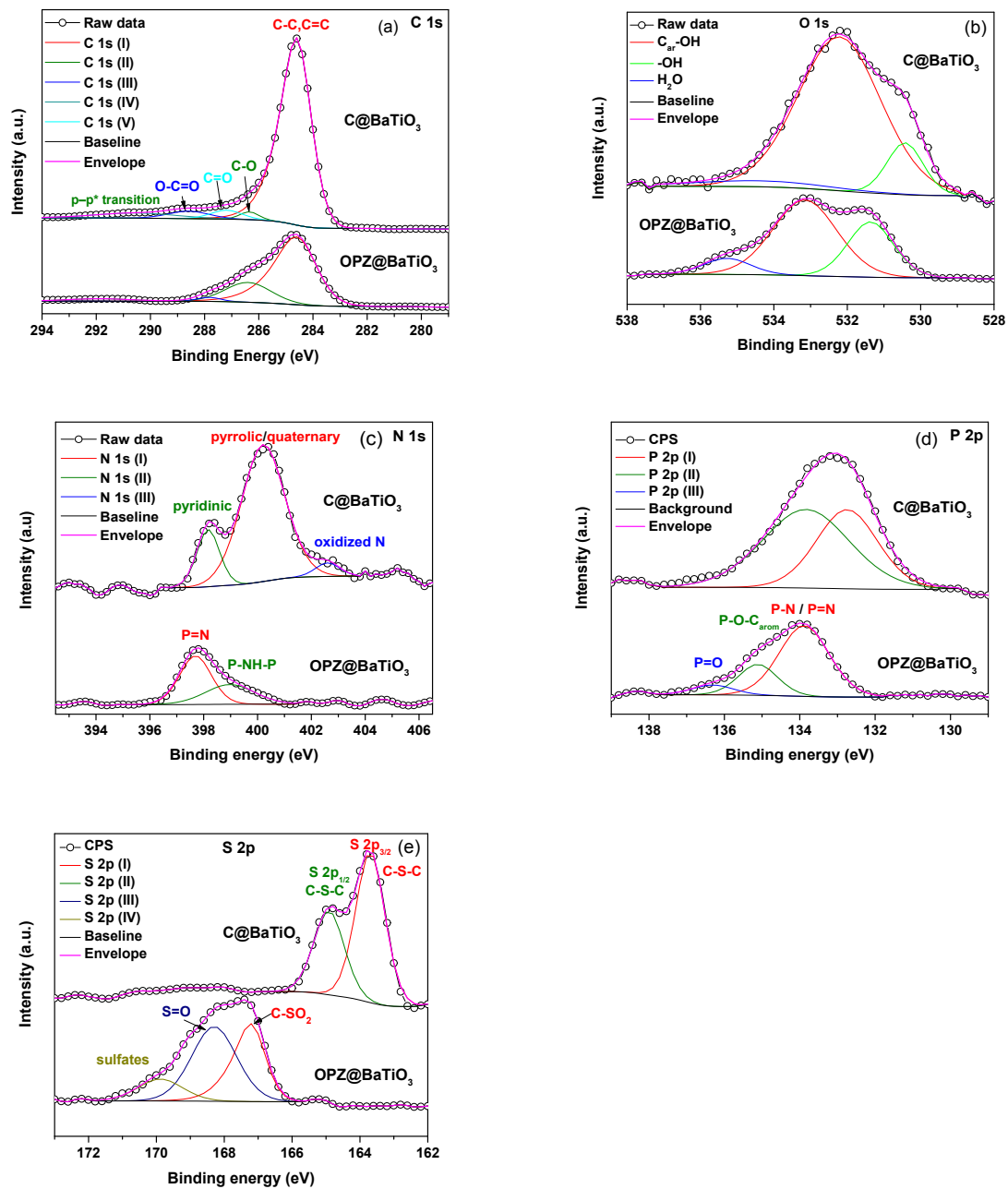


Figure S7. Core-level XPS scanning and deconvolution of the peaks of the core-shell particles before and after carbonization.

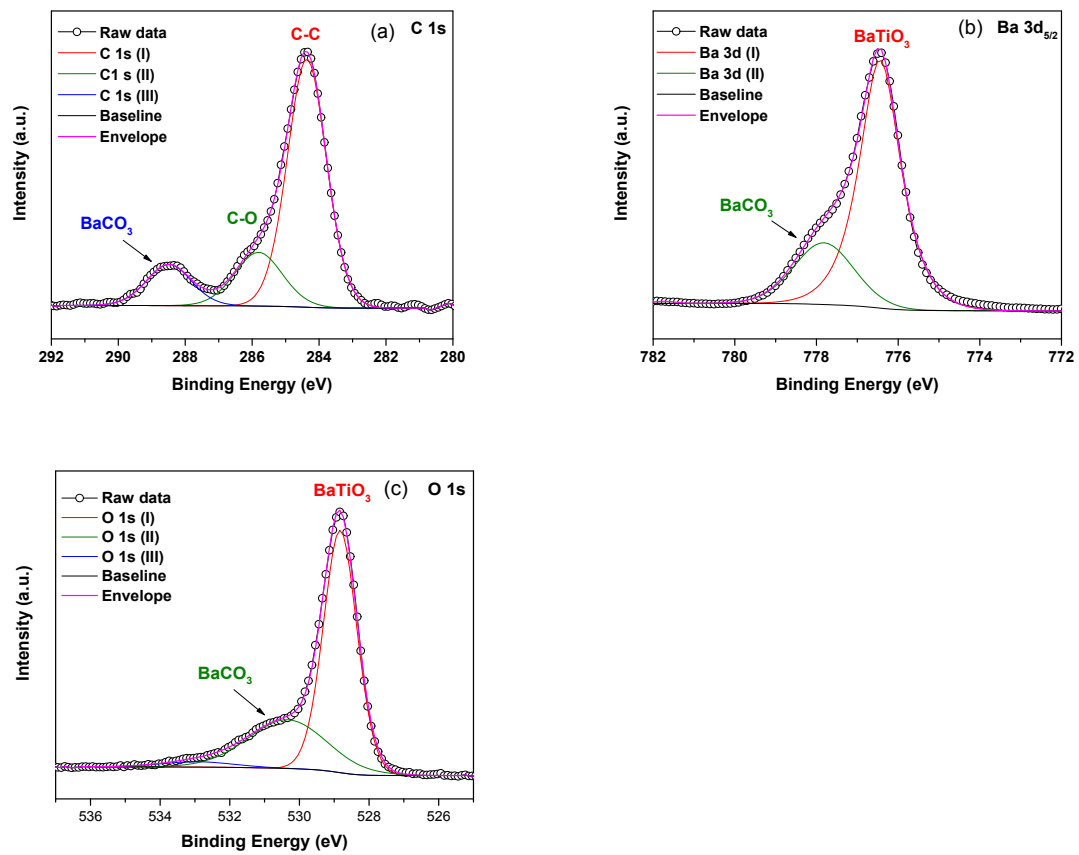


Figure S8. BaTiO₃ XPS core-level spectra of a) C 1s, b) Ba 3d_{5/2} and c) O 1s indicating the presence of BaCO₃